International Journal of Modern Physics A
© World Scientific Publishing Company

arXiv:2402.06993v1 [hep-th] 10 Feb 2024

2d (0,2) Gauge Theories from Branes: Recent Progress in Brane Brick Models

Sebastián Franco

Physics Department, The City College of the CUNY
160 Convent Avenue, New York, NY 10031, USA
Physics Program and Initiative for the Theoretical Sciences
The Graduate School and University Center, The City University of New York
365 Fifth Avenue, New York NY 10016, USA
sfranco@ccny.cuny.edu

We discuss the realization of $2d$ $(0,2)$ gauge theories in terms of branes focusing on Brane Brick Models, which are T-dual to D1-branes probing toric Calabi-Yau 4-folds. These brane setups fully encode the infinite class of $2d$ $(0,2)$ quiver gauge theories on the worldvolume of the D1-branes and substantially streamline their connection to the probed geometries. We review various methods for efficiently generating Brane Brick Models. These algorithms are then used to construct $2d$ $(0,2)$ gauge theories for the cones over all the smooth Fano 3-folds and two infinite families of Sasaki-Einstein 7-manifolds with known metrics. This note is based on the author's talk at the Gauged Linear Sigma Models @ 30 conference at the Simons Center for Geometry and Physics.

Keywords: $2d$ (0,2) Gauge Theories; D-branes; Calabi-Yau 4-Folds.

PACS numbers:

1. Introduction

Engineering quantum field theories in terms of String or M-Theory branes is a powerful approach for studying their dynamics, often providing alternative perspectives. D-branes probing singularities provide a platform for constructing interesting field theories in different dimensions. $4d$ $\mathcal{N}=1$ gauge theories on D3-branes probing singular toric Calabi-Yau (CY) 3-folds are the most thoroughly studied setups within this class. In this case, *brane tilings* significantly streamline the connection between the $4d$ gauge theories on the D3-branes and the probed geometry.[1,2]

In recent years, the study of $2d$ $(0,2)$ gauge theories on D1-branes probing toric CY 4-folds culminated with the introduction of *brane brick models*,[3] which result in powerful simplifications in the map between geometry and $2d$ theories analogous to the ones previously brought by brane tilings.

In this note, we present a brief review of recent works in which brane brick models have been exploited for determining and studying the gauge theories for large classes of interesting CY 4-folds. These geometries include the complex cones over all smooth Fano 3-folds,[4] and infinite families of cones over the $Y^{p,k}(\mathbb{CP}^1\times\mathbb{CP}^1)$

and $Y^{p,k}(\mathbb{CP}^2)$ Sasaki-Einstein 7-manifolds.[5]

2. Brane Brick Models

Brane brick models are obtained from D1-branes at CY_4 singularities by T-duality. We refer the reader to[3,6–8] for detailed discussions. A brane brick model is a Type IIA brane configuration consisting of D4-branes wrapping a 3-torus $\mathbb{T}^3$ and suspended from an NS5-brane that wraps a holomorphic surface Σ intersecting with $\mathbb{T}^3$. The holomorphic surface Σ is the zero locus of the Newton polynomial defined by the toric diagram of the CY_4. The basic ingredients of the brane setup are summarized in Table 1. The (246) directions are compactified on a $\mathbb{T}^3$. The $2d$ gauge theory lives on the two directions (01) common to all the branes.

Table 1. Brane brick model configuration.

	0	1	2	3	4	5	6	7	8	9
D4	×	×	×	·	×	·	×	·	·	·
NS5	×	×	——	——	Σ	——	——	——	·	·

Brane brick models, or equivalently their dual periodic quivers, fully encode the $2d$ $(0,2)$ quiver gauge theories on the worldvolume of D1-branes probing toric CY 4-folds. Namely, they summarize not only the quivers but also the J- and E-terms. The dictionary between brane brick models and gauge theories is summarized in Table 2.

Table 2. Dictionary between brane brick models and $2d$ $(0,2)$ gauge theories.

Brane Brick Model	**Gauge Theory**	**Periodic Quiver**
Brick	Gauge group	Node
Oriented face between bricks i and j	Bifundamental chiral field from node i to node j	Oriented (black) arrow from node i to node j
Unoriented square face between bricks i and j	Bifundamental Fermi field between nodes i and j	Unoriented (red) line between nodes i and j
Edge	J- or E-term	Plaquette encoding a J- or an E-term

For additional results regarding brane brick models, we refer the interested reader to.[9–11]

3. From CY_4's to Brane Brick Models

Several methods for constructing brane brick models associated to a given toric CY_4 have been developed. Some of them considerably simplify this task. Figure 1 summarizes a few of these procedures.

Partial resolution consists of embedding the toric diagram of interest within a larger toric diagram, for which the $2d$ gauge theory is known. A standard choice

for such initial geometry is an abelian orbifold of $\mathbb{C}^4$. The deletion of points that connects the two toric diagrams translates into higgsing in the field theory.[6] The determination of the chiral fields that acquire a non-zero VEV to achieve a desired toric diagram is simplified by considering the map between fields in the quiver and *brick matchings*, certain combinatorial objects in the associated brane brick model that are analogous to perfect matchings of brane tilings.[3]

Orbifold reduction generates the $2d$ $(0,2)$ gauge theories associated to D1-branes probing a toric CY_4 starting from $4d$ $\mathcal{N}=1$ gauge theories on D3-branes probing toric CY_3's or, equivalently, the corresponding brane tilings. Given two integers $k_+, k_- \geq 0$ and a perfect matching p_0 of a brane tilings for a CY_3, orbifold reduction generates a gauge theory that corresponds to a CY_4 whose toric diagram is obtained by expanding the point associated to p_0 into a line of length $k_+ + k_-$, with k_+ points above the original $2d$ toric diagram and k_-points below it. The algorithm for producing the $2d$ gauge theory has an elegant implementation in terms of the periodic quiver.[12] This procedure generalizes dimensional reduction and orbifolding. With orbifold reduction, the gauge theories for rather complicated CY_4's can be found with little effort.

$3d$ *printing* is similar to orbifold reduction in that it provides a combinatorial prescription for constructing the $2d$ (0,2) gauge theory for a CY_4 starting from the brane tiling for a CY_3.[13] In $3d$ printing, multiple points in the toric diagram of the CY_3 can be lifted to produce the toric diagram of the CY_4, as illustrated in Figure 1.

Mirror symmetry provides an alternative way for deriving the $2d$ $(0,2)$ gauge theory. The mirror configuration consists of D5-branes wrapping 4-spheres and the gauge theory is determined by how they intersect.[8,14] Figure 1, shows various projections that contribute to the visualization of the configuration of branes in the mirror. Interestingly, changing the complex structure and passing through vanishing cycles results in inequivalent geometries. However, the mirror geometry unifies the inequivalent geometries of the CY into a single CY manifold. In this way we can understand field theory dualities from the uniqueness of the CY mirror.

4. Fano 3-Folds

Brane brick models are particularly useful for finding the $2d$ (0,2) gauge theories for large families of toric CY 4-folds. An interesting family of geometries is given by the complex cones over Gorenstein Fano varieties that are constructed from a special set of lattice polytopes known as reflexive polytopes. Table 3 summarizes the numbers of inequivalent reflexive polytopes up to dimension 4, following the seminal classification of Kreuzer and Skarke.[15–17]

These polytopes should be regarded as the toric diagrams of toric CY's constructed as the complex cones over the corresponding Fanos. We are interested in CY 4-folds, i.e. dimension 3, where there are 4,319 polytopes. Moreover, let us focus on those reflexive polytopes that are also regular, which implies that their associ-

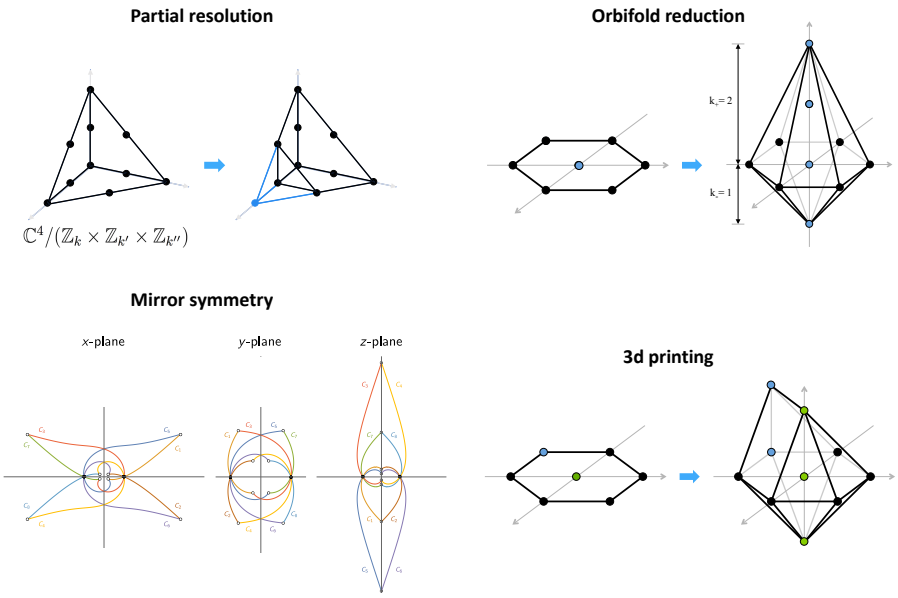

Fig. 1. Some methods for generating brane brick models for toric CY 4-folds.

Table 3. The number of inequivalent reflexive polytopes and regular reflexive polytopes in dimension $d \leq 4$.[15–17]

d	Number of Polytopes	Number of Regular Polytopes
1	1	1
2	16	5
3	4,319	18
4	473,800,776	124

ated Gorenstein Fano varieties are smooth. According to Table 2, this leaves us with a manageable subset of 18 polytopes, shown in Figure 2.

The CY_3 analogues of these geometries are the complex cones over F_0 and del Pezzo surfaces, which have played a prominent role in elucidating the correspondence between CY 3-folds and the $4d$ $\mathcal{N} = 1$ gauge theories on D3-branes probing them (see e.g.[18–21]).

In,[4] a brane brick model, i.e. a $2d$ $(0, 2)$ gauge theory, was constructed for each of the 18 regular reflexive polytopes in 3 dimensions. For every one of these models, the moduli space was thoroughly studied, calculating the generating function of mesonic gauge invariant operators, the Hilbert series, using the Molien integral formula. For each of these models, the generators of the mesonic moduli space were expressed both in terms of chiral fields of the $2d$ gauge theory as well as brick matchings. Finally, for all these models, it was verified that the generator lattice of the corresponding mesonic moduli space is the polar reflexive dual of the toric diagram.

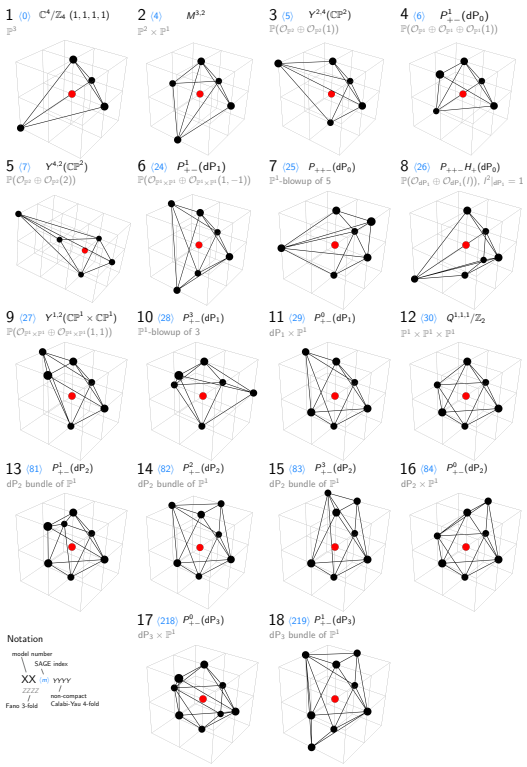

Fig. 2. The 18 regular reflexive polytopes in dimension 3 corresponding to toric non-compact CY 4-folds and corresponding smooth Fano 3-folds.

4.1. *An Example: Model 11*

To illustrate the results in,[4] let us focus on Model 11. Figure 3 shows how the toric diagram for this model can be connected to two different CY_3 toric diagrams. Therefore, it is possible to derive the corresponding $2d$ $(0,2)$ gauge theory using some of the approaches reviewed in Section 3. Starting from dP_1, the toric diagram for Model 11 is obtained by lifting the central point in two opposite directions. The associated gauge theory can be therefore constructed from the one for dP_1 using orbifold reduction. Alternatively, the toric diagram for Model 11 follows from lifting two points in the toric diagram of F_0. Consequently, the gauge theory for Model 11 can also be constructed by $3d$ printing starting from the gauge theory for F_0. It is interesting to reflect on how the $SU(2) \times SU(2)$ global symmetry of the final gauge theory arises from these two alternative constructions. In the first one, only one of the $SU(2)$ factors is present in dP_1, while the second one emerges from orbifold reduction. In contrast, the full $SU(2) \times SU(2)$ symmetry is already present in F_0.

The corresponding brane brick model has the quiver in Figure 4 and the J- and

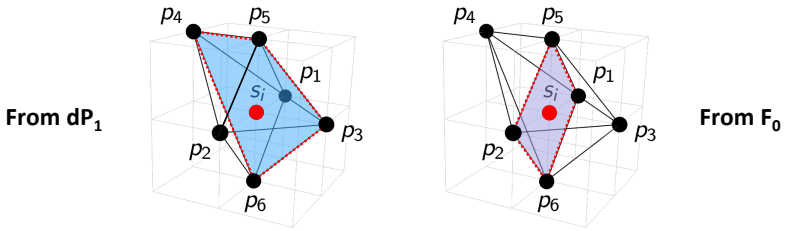

Fig. 3. Two alternative ways of obtaining the toric diagram for Model 11 from CY_3 toric diagrams.

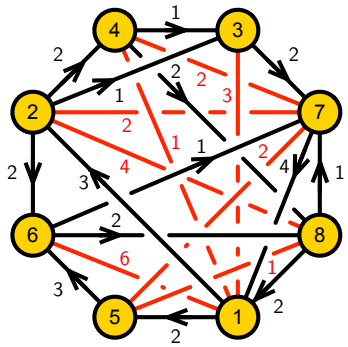

Fig. 4. Quiver for Model 11.

E-terms are

$$
\begin{array}{lrcll}
 & & J & & E \\
\Lambda^1_{16}: & Y_{68}X_{81} & - & X_{67}X_{71} & P_{15}X_{56} - X_{12}P_{26} \\
\Lambda^2_{16}: & X_{67}Y_{71} & - & X_{68}X_{81} & P_{15}Y_{56} - Y_{12}P_{26} \\
\Lambda^3_{16}: & X_{68}X_{87}X_{71} & - & Y_{68}X_{87}Y_{71} & P_{15}Z_{56} - Z_{12}P_{26} \\
\Lambda^4_{16}: & Y_{68}S_{81} & - & X_{67}S_{71} & X_{12}Q_{26} - Q_{15}X_{56} \\
\Lambda^5_{16}: & X_{67}T_{71} & - & X_{68}S_{81} & Y_{12}Q_{26} - Q_{15}Y_{56} \\
\Lambda^6_{16}: & X_{68}X_{87}S_{71} & - & Y_{68}X_{87}T_{71} & Z_{12}Q_{26} - Q_{15}Z_{56} \\
\Lambda^1_{27}: & Y_{71}Y_{12} & - & X_{71}X_{12} & P_{26}X_{67} - X_{23}P_{37} \\
\Lambda^2_{27}: & T_{71}Y_{12} & - & S_{71}X_{12} & X_{23}Q_{37} - Q_{26}X_{67} \\
\Lambda^1_{28}: & X_{87}X_{71}Z_{12} & - & X_{81}Y_{12} & P_{26}X_{68} - X_{24}P_{48} \\
\Lambda^2_{28}: & X_{81}X_{12} & - & X_{87}Y_{71}Z_{12} & P_{26}Y_{68} - Y_{24}P_{48} \\
\Lambda^3_{28}: & X_{87}S_{71}Z_{12} & - & S_{81}Y_{12} & X_{24}Q_{48} - Q_{26}X_{68} \\
\Lambda^4_{28}: & S_{81}X_{12} & - & X_{87}T_{71}Z_{12} & Y_{24}Q_{48} - Q_{26}Y_{68} \\
\Lambda^1_{31}: & Z_{12}X_{24}X_{43} & - & X_{12}X_{23} & P_{37}X_{71} - Q_{37}S_{71} \\
\Lambda^2_{31}: & Y_{12}X_{23} & - & Z_{12}Y_{24}X_{43} & P_{37}Y_{71} - Q_{37}T_{71} \\
\Lambda_{41}: & X_{12}Y_{24} & - & Y_{12}X_{24} & P_{48}X_{81} - Q_{48}S_{81} \\
\Lambda^1_{47}: & X_{71}Z_{12}X_{24} & - & Y_{71}Z_{12}Y_{24} & P_{48}X_{87} - X_{43}P_{37} \\
\Lambda^2_{47}: & S_{71}Z_{12}X_{24} & - & T_{71}Z_{12}Y_{24} & X_{43}Q_{37} - Q_{48}X_{87} \\
\Lambda^1_{75}: & Z_{56}X_{68}X_{87} & - & X_{56}X_{67} & S_{71}Q_{15} - X_{71}P_{15} \\
\Lambda^2_{75}: & Y_{56}X_{67} & - & Z_{56}Y_{68}X_{87} & T_{71}Q_{15} - Y_{71}P_{15} \\
\Lambda_{85}: & X_{56}Y_{68} & - & Y_{56}X_{68} & S_{81}Q_{15} - X_{81}P_{15}
\end{array}
\tag{1}
$$

Table 4 presents the generators of the mesonic moduli space of Model 11 in terms of brick matchings with the corresponding flavor charges. Figure 5 shows the corresponding generator lattice, which is a reflexive polytope that is the dual of the

toric diagram of Model 11 shown in Figure 2, as expected.

Table 4. The generators of the mesonic moduli space of Model 11 in terms of brick matchings with the corresponding flavor charges.

Generator	$SU(2)_{\tilde{x}}$	$SU(2)_{\tilde{y}}$	$U(1)_{\tilde{b}}$
$p_1^2p_3p_6^2$ so	1	0	-1
$p_1p_2p_3p_6^2$ so	0	0	-1
$p_2^2p_3p_6^2$ so	-1	0	-1
$p_1^2p_4p_6^2$ so	1	-1	-1
$p_1p_2p_4p_6^2$ so	0	-1	-1
$p_2^2p_4p_6^2$ so	-1	-1	-1
$p_1^2p_3^2p_5p_6$ so^2	1	1	0
$p_1p_2p_3^2p_5p_6$ so^2	0	1	0
$p_2^2p_3^2p_5p_6$ so^2	-1	1	0
$p_1^2p_3p_4p_5p_6$ so^2	1	0	0
$p_1p_2p_3p_4p_5p_6$ so^2	0	0	0
$p_2^2p_3p_4p_5p_6$ so^2	-1	0	0
$p_1^2p_4^2p_5p_6$ so^2	1	-1	0
$p_1p_2p_4^2p_5p_6$ so^2	0	-1	0
$p_2^2p_4^2p_5p_6$ so^2	-1	-1	0
$p_1^2p_3^3p_5^2$ so^3	1	2	1
$p_1p_2p_3^3p_5^2$ so^3	0	2	1
$p_2^2p_3^3p_5^2$ so^3	-1	2	1
$p_1^2p_3^2p_4p_5^2$ so^3	1	1	1
$p_1p_2p_3^2p_4p_5^2$ so^3	0	1	1
$p_2^2p_3^2p_4p_5^2$ so^3	-1	1	1
$p_1^2p_3p_4^2p_5^2$ so^3	1	0	1
$p_1p_2p_3p_4^2p_5^2$ so^3	0	0	1
$p_2^2p_3p_4^2p_5^2$ so^3	-1	0	1
$p_1^2p_4^3p_5^2$ so^3	1	-1	1
$p_1p_2p_4^3p_5^2$ so^3	0	-1	1
$p_2^2p_4^3p_5^2$ so^3	-1	-1	1

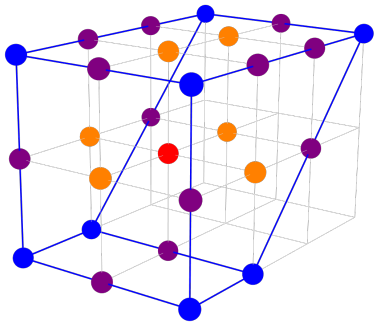

Fig. 5. Generator lattice for Model 11.

In,[4] all generators were also expressed in terms of chiral fields in the quiver. As

an example, Table 5 provides these expressions for the first two generators in Table 4. Every generator can be represented in multiple ways in terms of the fields in the gauge theory.

Table 5. First two generators in Table 4 expressed in terms of chiral fields in the quiver.

Generator	$SU(2)_{\tilde{x}}$	$SU(2)_{\tilde{y}}$	$U(1)_{\tilde{b}}$
$P_{15}Z_{56}X_{67}S_{71} = P_{15}Z_{56}Y_{68}S_{81} = Z_{12}P_{26}X_{67}S_{71} =$ $= Z_{12}P_{26}Y_{68}S_{81} = Z_{12}X_{23}P_{37}S_{71} = Z_{12}Y_{24}P_{48}S_{81}$	1	0	-1
$P_{15}Z_{56}X_{67}X_{71} = P_{15}Z_{56}Y_{68}X_{81} = Z_{12}P_{26}X_{67}X_{71} =$ $= Z_{12}P_{26}Y_{68}X_{81} = Z_{12}X_{23}P_{37}X_{71} = Z_{12}Y_{24}P_{48}X_{81}$	0	0	-1

5. Sasaki-Einstein 7-Manifolds

Every $2n$-dimensional Kähler-Einstein manifold B_{2n} there is an infinite family of compact Sasaki-Einstein (SE) manifolds Y_{2n+3} of dimension $2n+3$.[22,23] For $n = 2$, the 4-dimensional Kähler-Einstein bases B_4 are either $\mathbb{CP}^1 \times \mathbb{CP}^1$ or $\mathbb{CP}^2$, giving rise to two infinite families of SE 7-manifolds denoted $Y^{p,k}(\mathbb{CP}^1 \times \mathbb{CP}^1)$ and $Y^{p,k}(\mathbb{CP}^2)$, respectively. The two families stand out because their SE metrics are known explicitly.[22,23]

The general toric diagrams for the corresponding CY 4-folds are show in Figure 6[a], where the ranges for the parameters p and k are

$$\begin{aligned} Y^{p,k}(\mathbb{CP}^1 \times \mathbb{CP}^1) \quad &: \; 0 \leq k \leq p \; , \\ Y^{p,k}(\mathbb{CP}^2) \quad &: \; 0 \leq k \leq \tfrac{3}{2}p \; . \end{aligned} \tag{2}$$

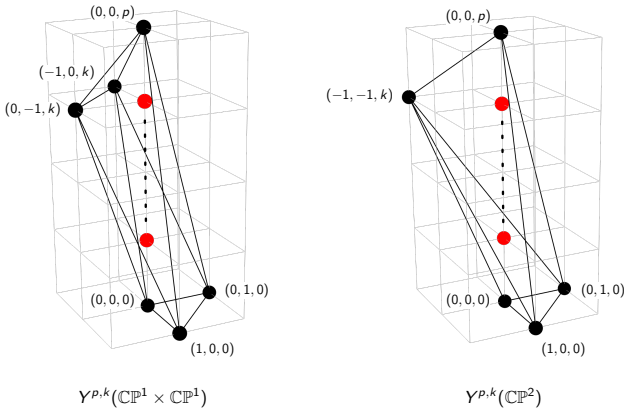

$Y^{p,k}(\mathbb{CP}^1 \times \mathbb{CP}^1)$ $Y^{p,k}(\mathbb{CP}^2)$

Fig. 6. General toric diagrams for the $Y^{p,k}(\mathbb{CP}^2)$ and $Y^{p,k}(\mathbb{CP}^1 \times \mathbb{CP}^1)$ families of toric CY 4-folds.

[a]For brevity, we use the name of the SE base to also identify the corresponding CY_4.

The isometry of the SE 7-manifolds takes the general form $H \times U(1)^2$, with H the isometry of the base B_4. For $Y^{p,k}(\mathbb{CP}^1 \times \mathbb{CP}^1)$ and $Y^{p,k}(\mathbb{CP}^2)$, the isometries are $SU(2) \times SU(2) \times U(1)^2$ and $SU(3) \times U(1)^2$, respectively. These isometries translate into the global symmetries of the corresponding $2d$ $(0,2)$ gauge theories.

The $2d$ $(0,2)$ gauge theories for both infinite families of CY 4-folds were constructed in,[5] guided by the techniques presented in Section 3. For example, the cones over $Y^{p,k}(\mathbb{CP}^2)$ with $p = \frac{2}{3}k = 2m$ and $m \in \mathbb{Z}^+$ are equivalent to abelian orbifolds of the form $M^{3,2}/\mathbb{Z}_m$. The corresponding $2d$ $(0,2)$ theories can be obtained via orbifold reduction of the $4d$ $\mathcal{N} = 1$ theory corresponding to dP_0. This is made clear by Figure 7, where the highlighted plane indicates the toric diagram for dP_0. While not all the $Y^{p,k}(\mathbb{CP}^2)$ theories can be constructed in this way, the models we obtain contain sufficient information to propose a closed form for the entire family, a proposal that can then be checked to be correct. The gauge theories for the full $Y^{p,k}(\mathbb{CP}^1 \times \mathbb{CP}^1)$ family can be determined using the same approach.

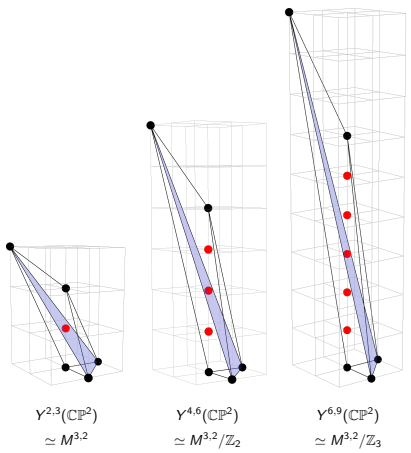

Fig. 7. Various $Y^{p,k}(\mathbb{CP}^2)$ geometries that can be obtained via orbifold reduction from dP_0.

As an example, the quiver for the $2d$ $(0,2)$ theory corresponding to $Y^{3,1}(\mathbb{CP}^2)$ is shown in Figure 8. The corresponding J- and E-terms take the following form

$$
\begin{array}{cll}
 & J & E \\
\Lambda^i_{12}: & \epsilon_{ijk} X^j_{23} X^k_{31} & P_{15} X^i_{56} Q_{62} - Q_{17} X^i_{72} \\
\Lambda^{2i}_{29}: & \epsilon_{ijk} X^j_{97} X^k_{72} & X^i_{23} Q_{39} - Q_{28} X^i_{89} \\
\Lambda^{2i}_{37}: & \epsilon_{ijk} X^j_{72} X^k_{23} & X^i_{31} Q_{17} - Q_{39} X^i_{97} \\
\Lambda^i_{45}: & \epsilon_{ijk} X^j_{56} X^k_{64} & X^i_{48} Q_{85} - Q_{43} X^i_{31} P_{15} \\
\Lambda^{2i}_{63}: & \epsilon_{ijk} X^j_{31} P_{15} X^k_{56} & X^i_{64} Q_{43} - Q_{62} X^i_{23} \\
\Lambda^i_{78}: & \epsilon_{ijk} X^j_{89} X^k_{97} & X^i_{72} Q_{28} - Q_{74} X^i_{48} \\
\Lambda^{2i}_{86}: & \epsilon_{ijk} X^j_{64} X^k_{48} & X^i_{89} Q_{96} - Q_{85} X^i_{56} \\
\Lambda^{2i}_{94}: & \epsilon_{ijk} X^j_{48} X^k_{89} & X^i_{97} Q_{74} - Q_{96} X^i_{64}
\end{array}
\quad , \tag{3}
$$

where $i, j, k = 1, 2, 3$ are $SU(3)$ global symmetry indices.

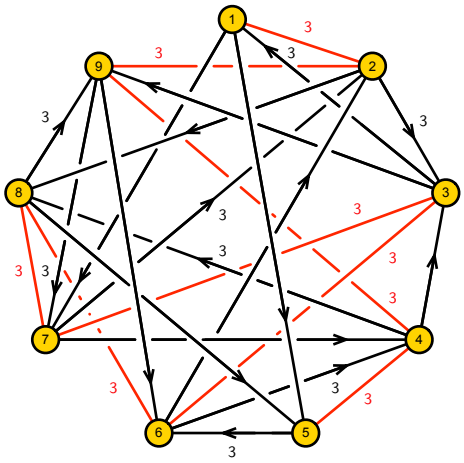

Fig. 8. Quiver for $Y^{3,1}(\mathbb{CP}^2)$.

Computing the moduli space of this theory, one obtains the toric diagram in Figure 9, which is indeed the one for $Y^{3,1}(\mathbb{CP}^2)$.

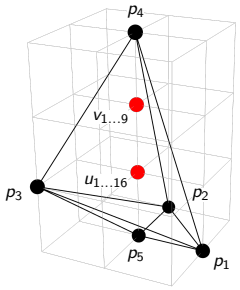

Fig. 9. Toric diagram of $Y^{3,1}(\mathbb{CP}^2)$.

Acknowledgments

It is a pleasure to thank the organizers of Gauged Linear Sigma Models @ 30 for putting together such an exciting meeting and for the opportunity to present my work. I would also like to acknowledge the staff at the Simons Center for Geometry and Physics for their wonderful hospitality. I am grateful to Dongwook Ghim and Rak-Kyeong Seong for enjoyable collaborations on the main works discussed in this presentation. This work is supported by the U.S. National Science Foundation grants PHY-2112729 and DMS-1854179.

References

1. S. Franco, A. Hanany, K. D. Kennaway, D. Vegh and B. Wecht, "Brane dimers and quiver gauge theories," JHEP **01**, 096 (2006) [arXiv:hep-th/0504110 [hep-th]].
2. S. Franco, A. Hanany, D. Martelli, J. Sparks, D. Vegh and B. Wecht, "Gauge theories from toric geometry and brane tilings," JHEP **01**, 128 (2006) [arXiv:hep-th/0505211 [hep-th]].
3. S. Franco, S. Lee and R. K. Seong, "Brane Brick Models, Toric Calabi-Yau 4-Folds and 2d (0,2) Quivers," JHEP **02**, 047 (2016) [arXiv:1510.01744 [hep-th]].
4. S. Franco and R. K. Seong, "Fano 3-folds, reflexive polytopes and brane brick models," JHEP **08**, 008 (2022) [arXiv:2203.15816 [hep-th]].
5. S. Franco, D. Ghim and R. K. Seong, "Brane brick models for the Sasaki-Einstein 7-manifolds $Y^{p,k}(\mathbb{CP}^1\times\mathbb{CP}^1)$ and $Y^{p,k}(\mathbb{CP}^2)$," JHEP **03**, 050 (2023) [arXiv:2212.02523 [hep-th]].
6. S. Franco, D. Ghim, S. Lee, R. K. Seong and D. Yokoyama, "2d (0,2) Quiver Gauge Theories and D-Branes," JHEP **09**, 072 (2015) [arXiv:1506.03818 [hep-th]].
7. S. Franco, S. Lee and R. K. Seong, "Brane brick models and 2d (0, 2) triality," JHEP **05**, 020 (2016) [arXiv:1602.01834 [hep-th]].
8. S. Franco, S. Lee, R. K. Seong and C. Vafa, "Brane Brick Models in the Mirror," JHEP **02**, 106 (2017) [arXiv:1609.01723 [hep-th]].
9. S. Franco, D. Ghim, S. Lee and R. K. Seong, "Elliptic Genera of 2d (0,2) Gauge Theories from Brane Brick Models," JHEP **06**, 068 (2017) [arXiv:1702.02948 [hep-th]].
10. S. Franco and X. Yu, "BFT_2: a general class of 2d$\mathcal{N}$ = (0, 2) theories, 3-manifolds and toric geometry," JHEP **08**, 277 (2022) [arXiv:2107.00667 [hep-th]].
11. S. Franco, D. Ghim, G. P. Goulas and R. K. Seong, "Mass deformations of brane brick models," JHEP **09**, 176 (2023) [arXiv:2307.03220 [hep-th]].
12. S. Franco, S. Lee and R. K. Seong, "Orbifold Reduction and 2d (0,2) Gauge Theories," JHEP **03**, 016 (2017) [arXiv:1609.07144 [hep-th]].
13. S. Franco and A. Hasan, "3d printing of 2d $\mathcal{N} = (0, 2)$ gauge theories," JHEP **05**, 082 (2018) [arXiv:1801.00799 [hep-th]].
14. M. Futaki and K. Ueda, "Tropical Coamoeba and Torus-Equivariant Homological Mirror Symmetry for the Projective Space," Commun. Math. Phys. **332**, no.1, 53-87 (2014)
15. M. Kreuzer and H. Skarke, "On the classification of reflexive polyhedra," Commun. Math. Phys. **185**, 495-508 (1997) [arXiv:hep-th/9512204 [hep-th]].
16. M. Kreuzer and H. Skarke, "Classification of reflexive polyhedra in three-dimensions," Adv. Theor. Math. Phys. **2**, 853-871 (1998) [arXiv:hep-th/9805190 [hep-th]].
17. M. Kreuzer and H. Skarke, "Complete classification of reflexive polyhedra in four-dimensions," Adv. Theor. Math. Phys. **4**, 1209-1230 (2000) [arXiv:hep-th/0002240 [hep-th]].
18. B. Feng, A. Hanany and Y. H. He, "D-brane gauge theories from toric singularities and toric duality," Nucl. Phys. B **595**, 165-200 (2001) [arXiv:hep-th/0003085 [hep-th]].
19. B. Feng, A. Hanany and Y. H. He, "Phase structure of D-brane gauge theories and toric duality," JHEP **08**, 040 (2001) [arXiv:hep-th/0104259 [hep-th]].
20. C. E. Beasley and M. R. Plesser, "Toric duality is Seiberg duality," JHEP **12**, 001 (2001) [arXiv:hep-th/0109053 [hep-th]].
21. B. Feng, S. Franco, A. Hanany and Y. H. He, "Symmetries of toric duality," JHEP **12**, 076 (2002) [arXiv:hep-th/0205144 [hep-th]].
22. J. P. Gauntlett, D. Martelli, J. F. Sparks and D. Waldram, "A New infinite class of Sasaki-Einstein manifolds," Adv. Theor. Math. Phys. **8**, no.6, 987-1000 (2004) [arXiv:hep-th/0403038 [hep-th]].

23. D. Martelli and J. Sparks, "Notes on toric Sasaki-Einstein seven-manifolds and AdS(4)/CFT(3)," JHEP **11**, 016 (2008) [arXiv:0808.0904 [hep-th]].